APPLICATION OF THE TRAJECTORY-GENERATED LOW-DIMENSIONAL MANIFOLD METHOD TO PREMIXED COMBUSTION OF METHANE

by

S. B. Pope

FDA 93-10 December 24, 1993

INTRODUCTION

Pope & Maas (1993) describe the trajectory-generated low-dimensional manifold (TGLDM) method for simplifying combustion chemistry, and they describe successful tests for a CO/H_2/air mixture. The tests are for a transient perfectly-stirred reactor, and the results show that the 2D method performs well both for major and minor species.

The method has also been applied to a methane-air mixture with less satisfactory results. The purpose of this report is to describe these tests.

MANIFOLD

The mixture is stoichiometric methane and air with an initial temperature of 1200K, and pressure of 1 bar.

The 2D TGLDM is generated as described by Pope & Maas (1993). The "major" species are taken to be H_2O, CO_2, N_2, O_2, CH_4 and CO. The remaining 10 species considered are, therefore "minor", including H_2, OH, O and H.

Figure 1 shows a projection of the manifold. The solid lines are reaction trajectories; and the mixing and equilibrium points are shown. The bold line is the 1D TGLDM, i.e. the reaction trajectory from the mixing point. A distinctive feature of the 2D manifold is the "fin". Reaction trajectories (from close to the mixing point) go up one side of the fin and down the other before reaching the equilibrium point. In fact, a closer visualization of the manifold projected into 3D, shows that the trajectories pass through the fin, i.e. the projection of the manifold intersects itself.

The qualitatively different performance of the 2D TGLDM method for methane compared to CO/H_2 is attributable to the shape of the methane manifold.

TESTS

The tests performed compare the performance of the TGLDM method with the detailed kinetics for the solution of the set of ordinary differential equa-

tions:

$$\frac{d\phi(t)}{dt} = \mathrm{S}(\phi(t)) - (\phi(t) - \phi^r)\omega, \tag{1}$$

with the initial condition

$$\phi(0) = \phi^0. \tag{2}$$

Here $\phi(t)$ is the specific mole number vector, and S is the rate of change of ϕ due to reaction. The final term in Eq. (1) is the perturbation and corresponds to a relaxation towards ϕ^r at a rate ω. There are six tests (numbered illogically) that correspond to different specifications of ϕ^r, ϕ^0 and ω. The values are given in Table 1.

Table 1: Test Conditions

Test Number	Description	ϕ^0	ϕ^r	$\omega(s^{-1})$
1	Reaction Trajectory	ϕ^{01}	ϕ^e	10^{-4}
2	PaSR	ϕ^m	ϕ^e	10^4
3	PaSR	ϕ^m	ϕ^e	10^8
4	PSR	ϕ^e	ϕ^m	10^4
5	PSR	ϕ^e	ϕ^m	10^{10}
6	PSR	ϕ^e	ϕ^m	10^2

ϕ^e – equilibrium
ϕ^m – mixing (i.e. unburnt mixture)
ϕ^{01} – composition approximately 1/3 along the trajectory produced by Test 2.

Test 4: PSR ($\omega = 10^4 s^{-1}$)

This test is identical (apart from the fuel) to the PSR test used by Pope & Maas (1993). The rate ω is $10^4 s^{-1}$, corresponding to a residence time of 0.1 ms.

For selected species, Figure 2 shows the time evolution of specific mole numbers. (In this and subsequent figures, the detailed calculation is the smoother of the two curves: the roughness in the TGLDM curve is due to numerical imperfections.) Figures 2a and 2b are typical of the other major

species, showing a significant difference between the two methods. Minor species are shown on Figs. 2c and 2d. Evidently the behavior of OH is qualitatively and quantitatively incorrect.

There is little doubt that the poor behavior for this case stems from the shape of the manifold close to equilibrium. Because of the "fin", the perturbation vector $\omega(\phi - \phi^r)$ has a significant component that is not in the tangent plane of the manifold.

Test 2: PaSR ($\omega = 10^4 s^{-1}$)

This test simulates part of the PaSR of Correa (1993). It may also be viewed as the converse of the previous test (Test 4): that is, with $\phi(0) = \phi^m$, the mixture relaxes to $\phi^r = \phi^e$.

The evolution of selected species is shown on Fig. 3. In this case the agreement appears much better. The main discrepancy appears to be that the TGLDM calculations "take off" a little bit more slowly, and so the profiles are shifted to the right.

The same data is shown on Fig. 4, but with the specific mole numbers plotted against $1 - e^{-\omega t}$. If there were no reaction, just mixing, then the detailed calculations would produce a straight line on this plot. Hence departures from linear behavior are a result of reaction.

Test 3: PaSR ($\omega = 10^8 s^{-1}$)

In order to study further the discrepancies in the previous test case, two further tests were performed (Tests 3 and 1) to isolate mixing and reaction, respectively.

Test 3 is the same as the previous test (Test 2) except that the mixing rate is set to the very large value $\omega = 10^8 s^{-1}$, so that most reaction rates are small in comparison. The evolution of species is shown on Fig. 5.

For pure mixing ($\omega \to \infty$) the trajectory given by the detailed calculation is the straight line between the mixing point and the equilibrium point. It may be seen from Fig. 5 that indeed the detailed calculation yields results extremely close to this straight line. For H_2O (Fig. 5a) and also for CO_2, O_2 and CH_4 (not shown) the TGLDM curve is quite close to the straight line. But for CO, and progressively more so for H_2 and OH, the TGLDM results show marked departures. This is simply because the manifold does not contain the straight line between ϕ^m and ϕ^e. This does not indicate a failure of the manifold method: for the method is intended to work only when ω is

small compared to the fast reaction rates.

Test 1: Reaction Trajectory

In this case ω is essentially zero ($\omega = 10^{-4}s^{-1}$), and so it amounts to a reaction trajectory calculation. Since the initial composition ϕ^{01} is on the manifold, the TGLDM method should give exactly the same result as the detailed calculation.

The results are shown on Fig. 6. It may be seen that there is near-perfect agreement during the large initial transient ($t < 10^{-4}s$). Subsequently, there is still good agreement, but the TGLDM method displays errors of around 5%. It is believed that these are simply numerical inaccuracies—e.g. interpolation errors. Presumably, these errors can be reduced at will by using finer tables etc.

Test 6: PSR ($\omega = 10^2 s^{-1}$)

For the final two tests we return to the PSR (Test 4), but with different values of ω. Here (Test 6) we consider the smaller value $\omega = 10^2 s$, i.e. a residence time of 10ms. The results are shown on Fig. 7.

As expected with the relatively large residence time, the departures from equilibrium are quite small (e.g. 1% for H_2O, 4% for CO, 5% for H_2). But for every species, the TGLDM method shows the wrong trend. It is likely that, because of the projection of the perturbation, the TGLDM trajectory is going in the wrong direction along the manifold.

(The ragged nature of the TGLDM curves for $t > 10^{-3}s$ indicates that the solution does not approach a stable fixed point, but exhibits (apparently) chaotic motion. This may be a numerical artifact.)

Test 5: PSR ($\omega = 10^{10} s^{-1}$)

This is the PSR test with $\omega = 10^{10} s^{-1}$. The solution given by the detailed scheme is simply that there is rapid mixing until the mixing composition is reached: reaction has a negligible effect. This, then, is the converse of Test 3. The trajectory followed by the detailed scheme is the straight line originating at ϕ^e and terminating at ϕ^m.

The results (Fig. 8) show that the TGLDM method gives a radically different result: a fixed point corresponding to stable combustion is attained. Presumably at this fixed point, the perturbation is almost perpendicular to

the manifold, so that its projection is much smaller than ω.

DISCUSSION AND CONCLUSIONS

1. The results are consistent with the correct implementation of the 2D TGLDM method. That is, there is no evidence of a gross error. The parametrization of the manifold is successful, even though there is a "fin". Almost certainly, a parametrization based on a simple projection would not be successful. Numerical inaccuracies are evident (e.g. Fig. 6), but do not invalidate the conclusions that can be drawn.

2. It appears that for CO/H_2 the 2D manifold is close to plane, whereas for CH_4 it certainly is not. A plane manifold has the special property that all perturbation vectors live in the tangent plane of the manifold. Hence the projection is the identity, and the TGLDM method becomes exact.

3. The performance of the TGLDM method for Test 5 (and for Test 3 for minor species) is simply wrong. But these tests are for very large ω, for which case manifold method are not intended to work. The conclusion from these tests, then, is simply a reminder and a warning: for non-plane manifolds, manifold methods should not be expected to work for large perturbations.

4. The performance of the 2D TGLDM method on the PSR Tests 4 and 6 is certainly disappointing, and requires further investigation. For sufficiently small ω, a manifold method should work well. An examination of the eigenvalues at equilibrium is needed to determine what is sufficiently small. But it is likely that $\omega = 10^2 s^{-1}$ (i.e. Test 6) is sufficiently small.

5. The theory of manifold methods clearly indicates that the eigenvector projection introduced by Maas & Pope (1992) is the correct projection to use. The perpendicular projection used here instead may account for the poor performance of the method for Test 6.

6. We now make some observations concerning the perturbation term. Consider a laminar flame. The perturbation arises from the diffusion

term, which is (approximately) $\nabla^2\phi$.

Now for a two-dimensional manifold $\boldsymbol{\Phi}(u,v)$, we have:

$$\nabla^2\boldsymbol{\Phi}(u,v) = \boldsymbol{\Phi}_u\nabla^2 u + \boldsymbol{\Phi}_v\nabla^2 v$$
$$+\boldsymbol{\Phi}_{uu}\nabla u\cdot\nabla u + 2\boldsymbol{\Phi}_{uv}\nabla u\cdot\nabla v + \boldsymbol{\Phi}_{vv}\nabla v\cdot\nabla v. \qquad (3)$$

It is important to appreciate the different properties of the first two and the last three terms. The first two terms, being a linear combination of the tangent vectors $\boldsymbol{\Phi}_u$ and $\boldsymbol{\Phi}_v$, lie in the tangent plane of the manifold. Hence this part of the perturbation can be handled without approximation.

The last three terms depend on the second derivatives of the manifold. At a point on the manifold where it is locally plane, these terms are zero. Hence we reach the important conclusion:

> At points on the manifold where the manifold is locally plane, perturbations arising from convection and diffusion are in the tangent plane, and hence are treated exactly in manifold methods, however the projection is chosen.

Conversely, the greatest errors in the approximation of the perturbation are likely to arise at locations where the manifold is strongly curved.

7. The tests employed here arise from PSR and PaSR concepts, and they may also be fair tests of the IEM turbulent mixing model. However, it should be recognized that the perturbation in the test does not have the property described above in Item 6. That is, where the manifold is locally plane, the perturbation does not lie in the tangent plane.

FUTURE WORK

The logical next step is to replace the perpendicular projection by the eigenvector projection. The method should then be accurate for the PSR test with sufficiently small ω. (It is not necessary to generate a whole manifold to perform this test. All that is required is the Jacobian at equilibrium.)

If the 2D TGLDM still yields poor performance for reasonable values of ω, there seems to be no alternative but to go to a 3D manifold.

REFERENCES

Correa, S.M. (1993) Combust. Flame **93**, 41.

Maas, U. and Pope, S.B. (1992) Twenty-Fourth Symposium (International) on Combustion, The Combustion Institute, p. 103.

Pope, S.B. and Maas, U. (1993) "Simplifying Chemical Kinetics: Trajectory-Generated Low-Dimensional Manifolds," submitted to the Twenty-Fifth Symposium (International) on Combustion.

FIGURE LEGENDS

Fig. 1: The 2D TGLDM for methane-air. Equilibrium point □; mixing point □; lines—reaction trajectories.

Fig. 2: Test 4, PSR ($\omega = 10^4 s^{-1}$). Specific mole numbers x1,000 vs. $\log_{10}(t)$, where t is in seconds. Comparison of detailed kinetics and TGLDM. a) H_2O, b) CO, c) H_2, d) OH.

Fig. 3: Test 2, PaSR ($\omega = 10^4 s^{-1}$). Specific mole numbers x1,000 vs. $\log_{10}(t)$, where t is in seconds. Comparison of detailed kinetics and TGLDM. a) H_2O, b) CO, c) H_2, d) OH.

Fig. 4: Test 2, PaSR ($\omega = 10^4 s^{-1}$). Specific mole number x1,000 vs. $1-e^{-wt}$. Comparison of detailed kinetics and TGLDM. a) H_2O, b) CO, c) H_2, d) OH.

Fig. 5: Test 3, PaSR ($\omega = 10^8 s^{-1}$). Specific mole number x1,000 vs. $1-e^{-wt}$. Comparison of detailed kinetics and TGLDM. a) H_2O, b) CO, c) H_2, d) OH.

Fig. 6 Test 1, Reactive Trajectory ($\omega = 10^4 s^{-1}$). Specific mole numbers x1,000 vs. $\log_{10}(t)$, where t is in seconds. Comparison of detailed kinetics and TGLDM. a) H_2O, b) CO, c) H_2, d) OH.

Fig. 7 Test 6, PSR ($\omega = 10^2 s^{-1}$). Specific mole numbers x1,000 vs. $\log_{10}(t)$, where t is in seconds. Comparison of detailed kinetics and TGLDM. a) H_2O, b) CO, c) H_2, d) OH.

Fig. 8 Test 5, PSR ($\omega = 10^{10} s^{-1}$). Specific mole numbers x1,000 vs. $\log_{10}(t)$, where t is in seconds. Comparison of detailed kinetics and TGLDM. a) H_2O, b) CO, c) H_2, d) OH.

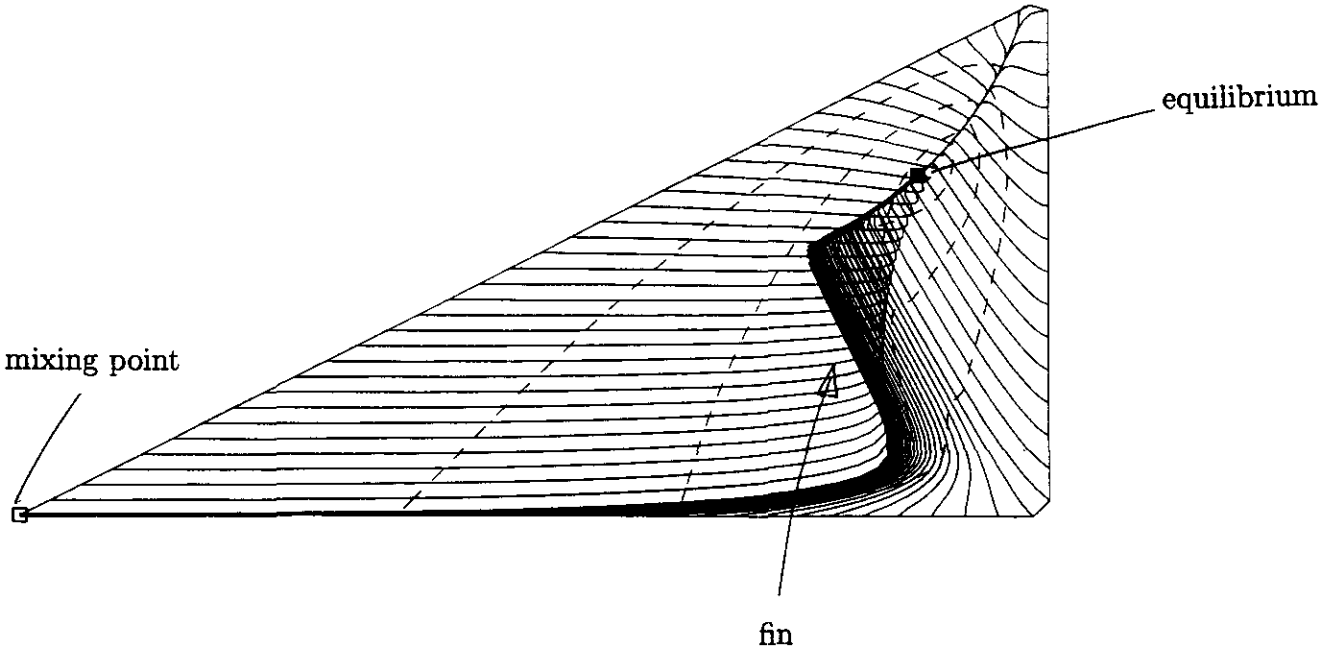

Fig. 1: The 2D TGLDM for methane-air. Equilibrium point ■; mixing point □; lines—reaction trajectories.

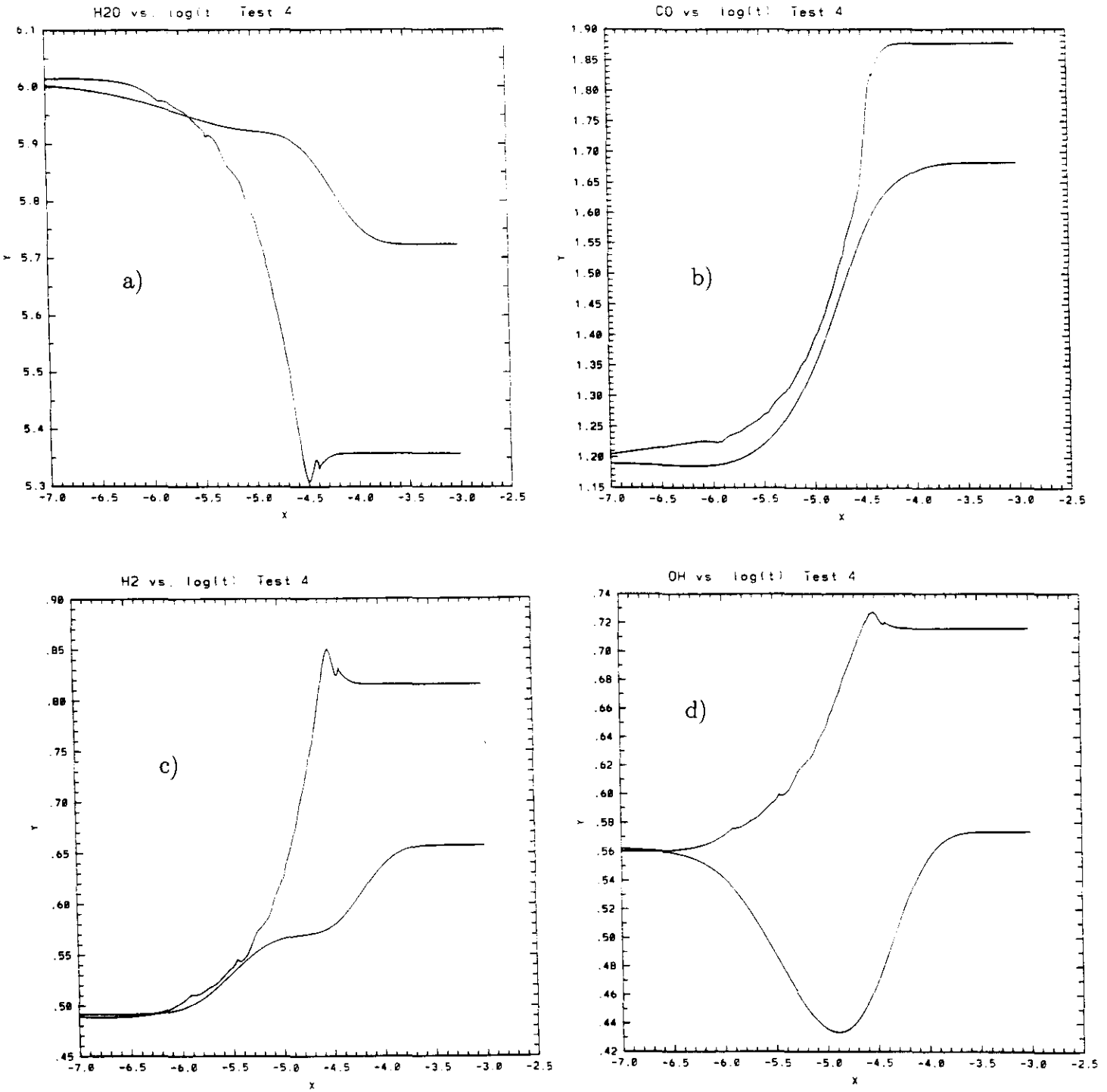

Fig. 2: Test 4, PSR ($\omega = 10^4 s^{-1}$). Specific mole numbers x1,000 vs. $\log_{10}(t)$, where t is in seconds. Comparison of detailed kinetics and TGLDM. a) H_2O, b) CO, c) H_2, d) OH.

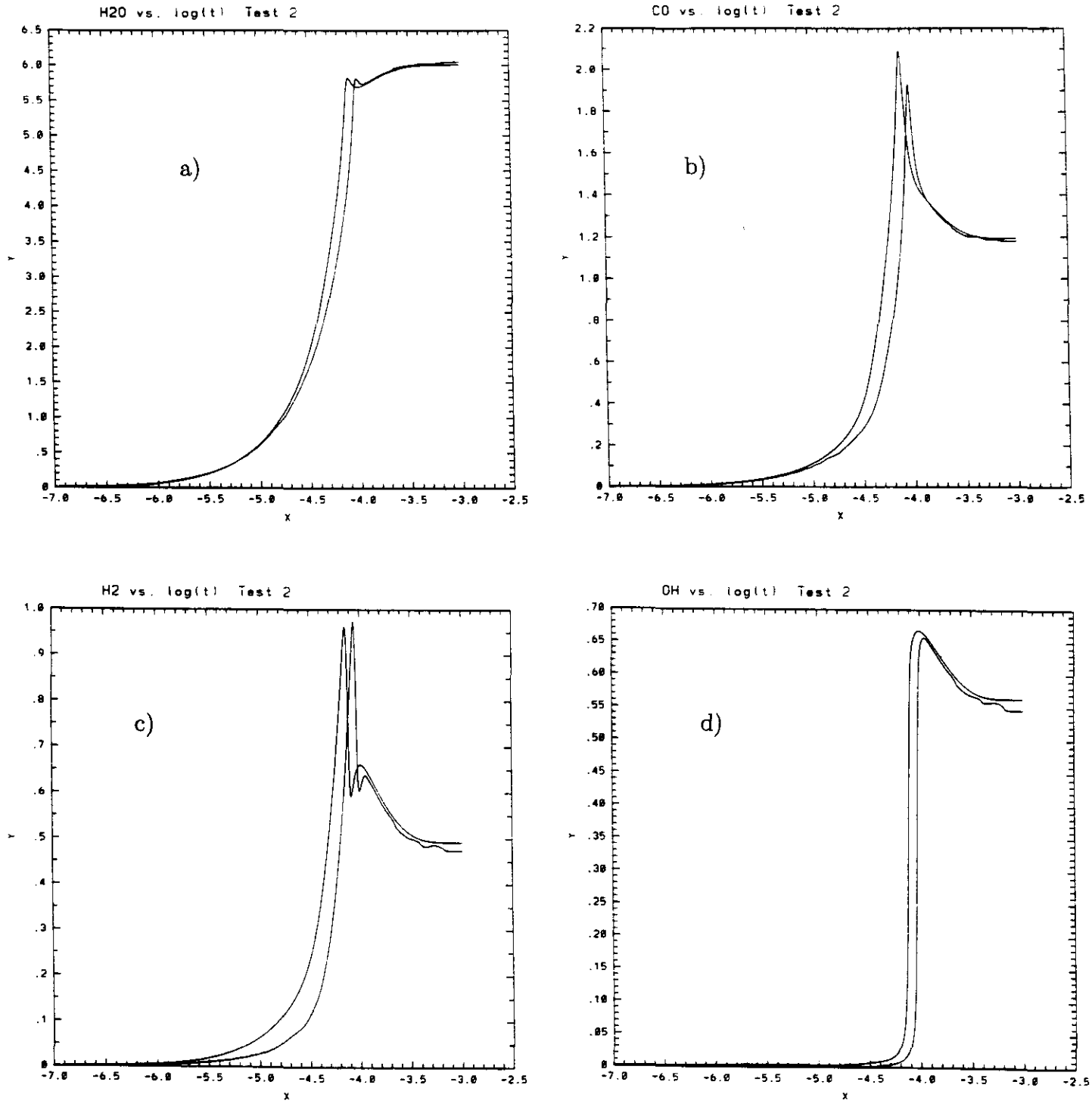

Fig. 3: Test 2, PaSR ($\omega = 10^4 s^{-1}$). Specific mole numbers x1,000 vs. $\log_{10}(t)$, where t is in seconds. Comparison of detailed kinetics and TGLDM. a) H_2O, b) CO, c) H_2, d) OH.

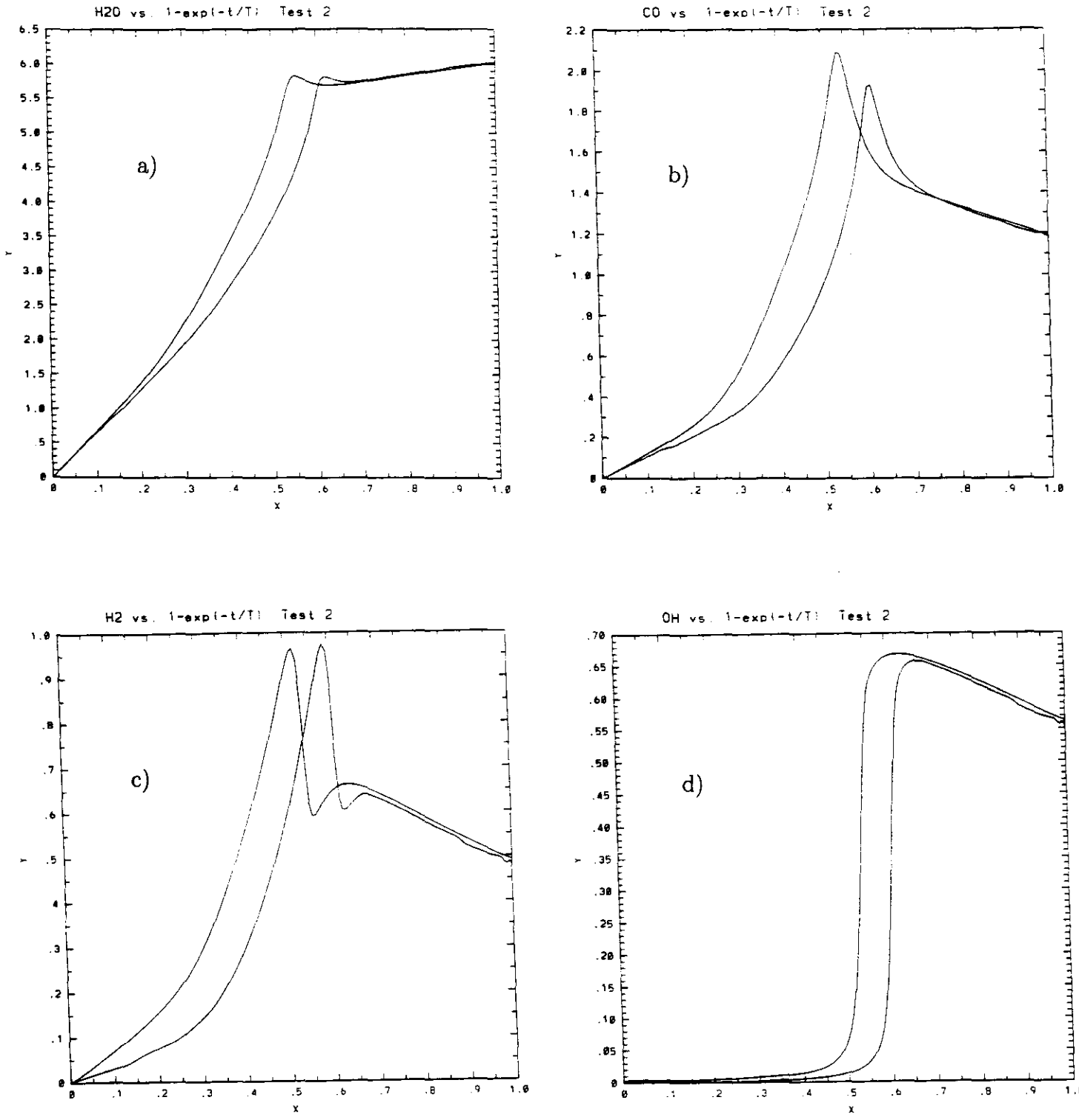

Fig. 4: Test 2, PaSR ($\omega = 10^4 s^{-1}$). Specific mole number x1,000 vs. $1-e^{-wt}$. Comparison of detailed kinetics and TGLDM. a) H_2O, b) CO, c) H_2, d) OH.

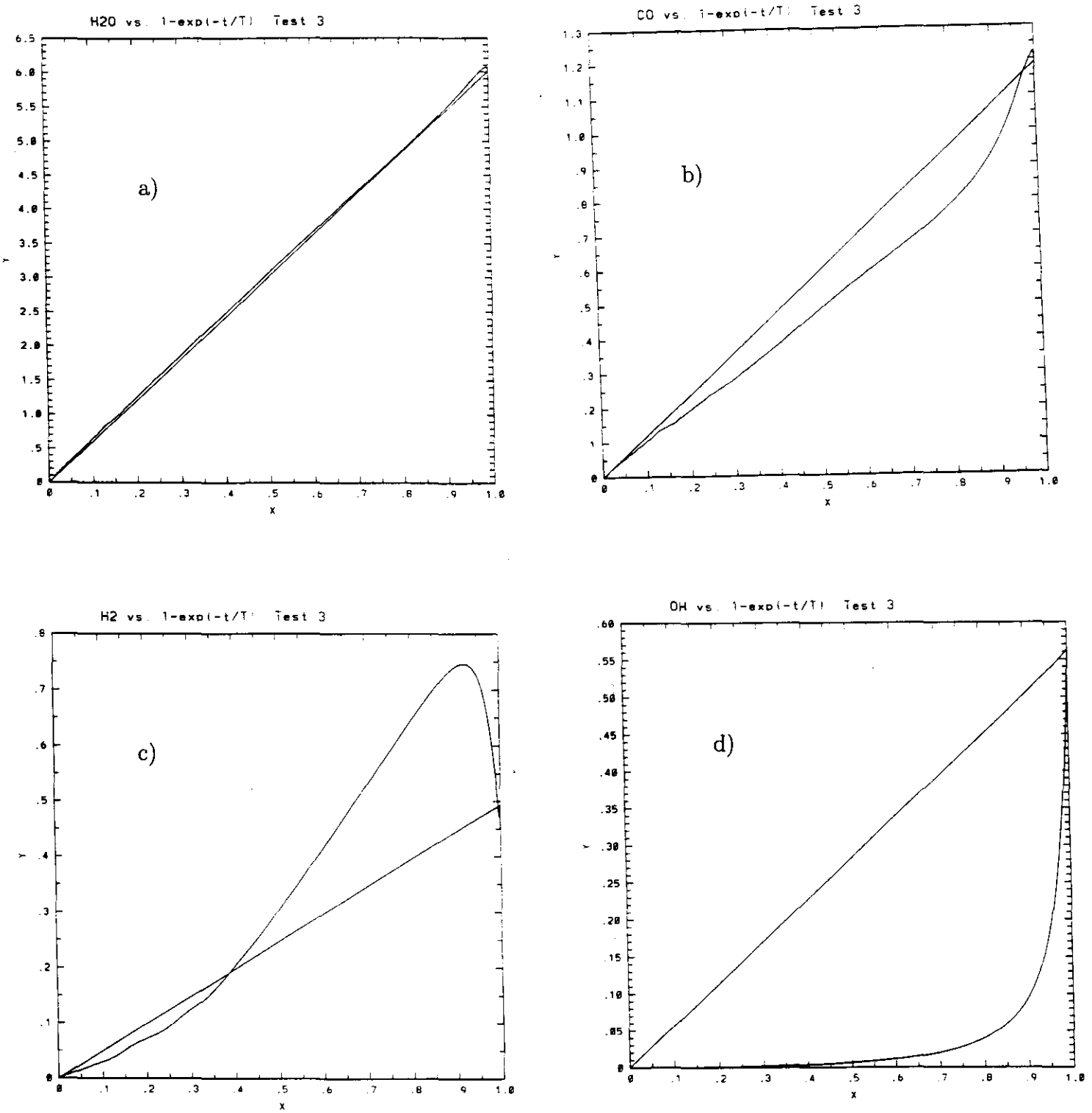

Fig. 5: Test 3, PaSR ($\omega = 10^8 s^{-1}$). Specific mole number x1,000 vs. $1-e^{-wt}$. Comparison of detailed kinetics and TGLDM. a) H_2O, b) CO, c) H_2, d) OH.

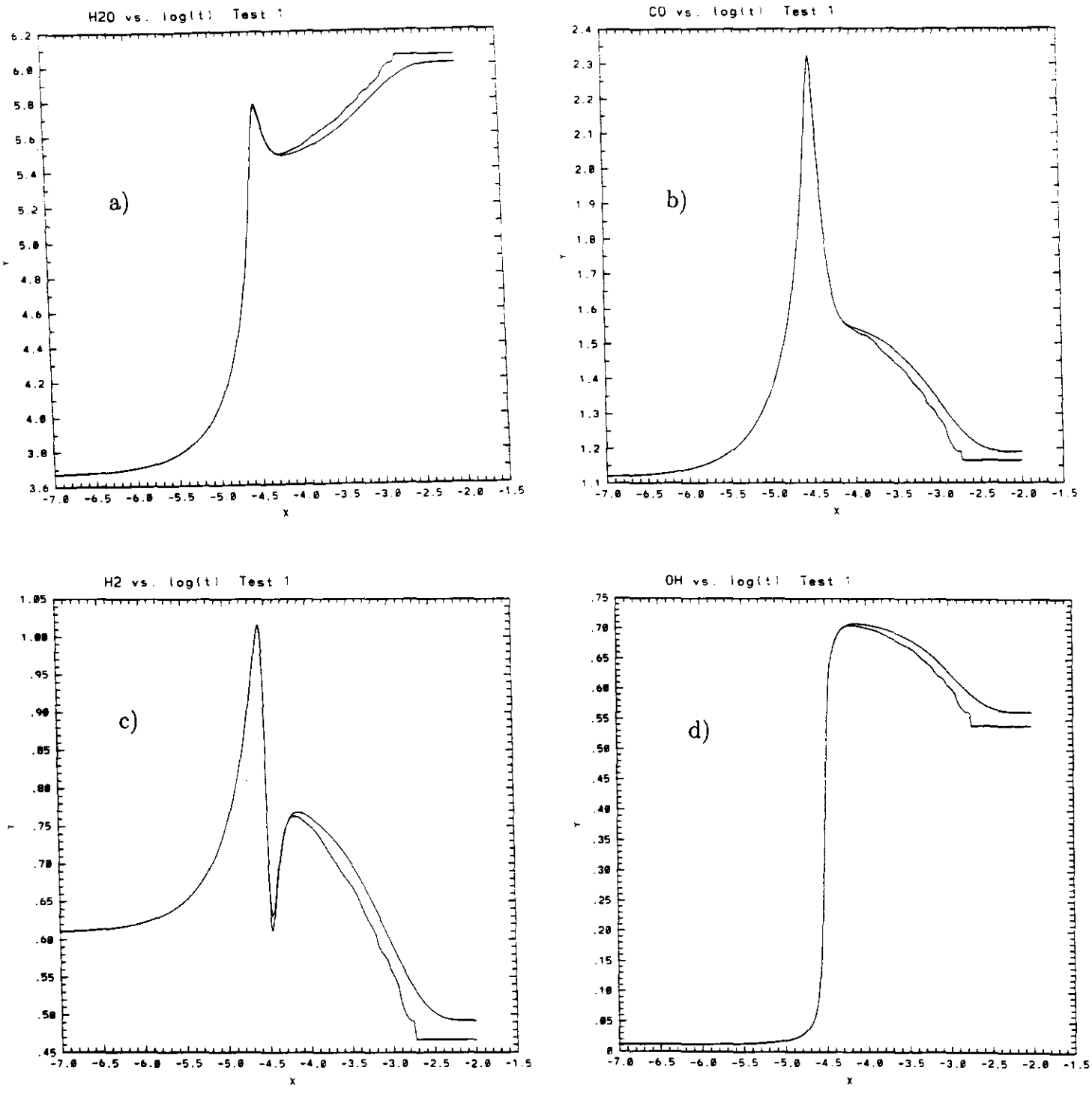

Fig. 6 Test 1, Reactive Trajectory ($\omega = 10^4 s^{-1}$). Specific mole numbers x1,000 vs. $\log_{10}(t)$, where t is in seconds. Comparison of detailed kinetics and TGLDM. a) H_2O, b) CO, c) H_2, d) OH.

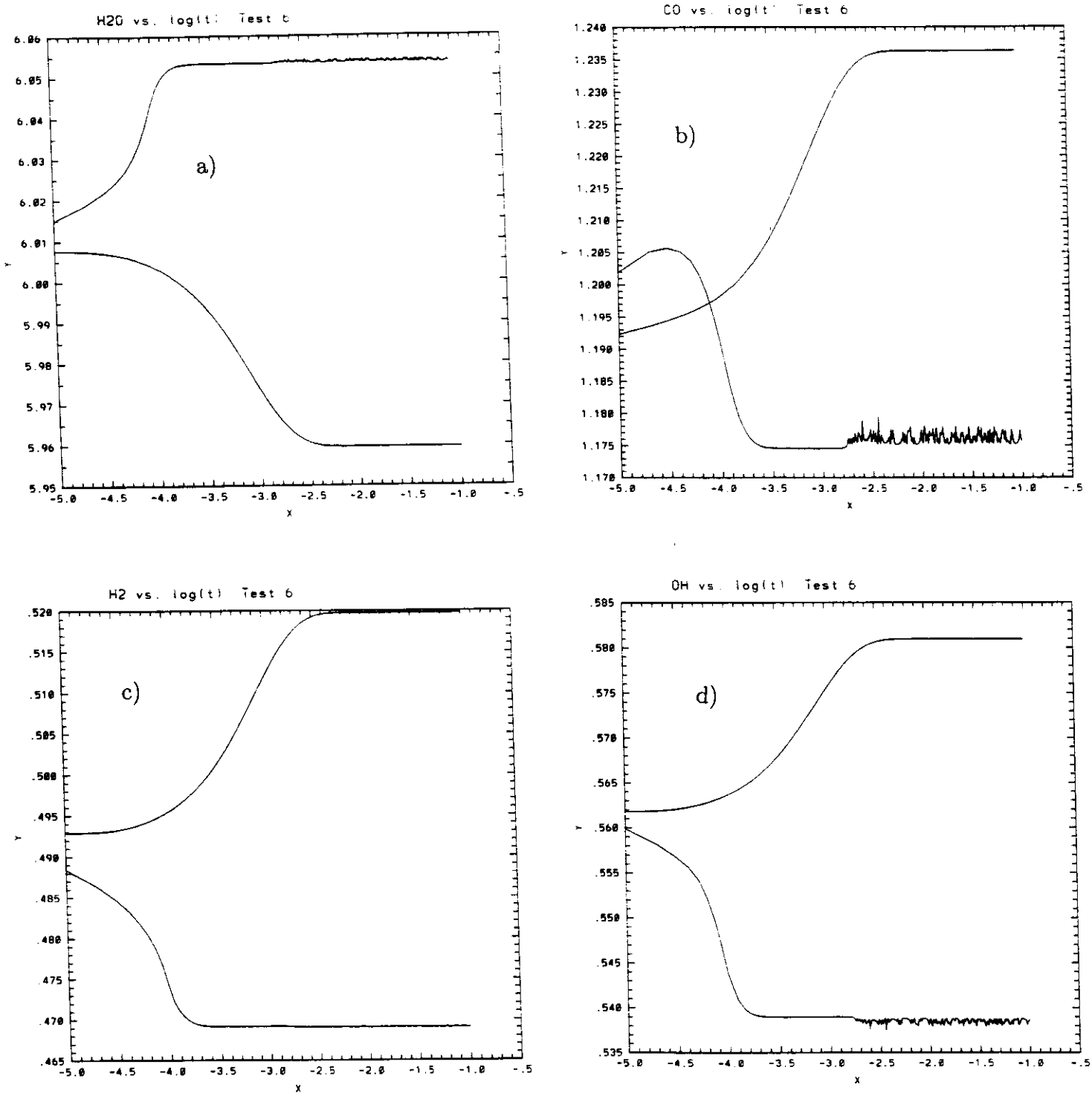

Fig. 7 Test 6, PSR ($\omega = 10^2 s^{-1}$). Specific mole numbers x1,000 vs. $\log_{10}(t)$, where t is in seconds. Comparison of detailed kinetics and TGLDM. a) H_2O, b) CO, c) H_2, d) OH.

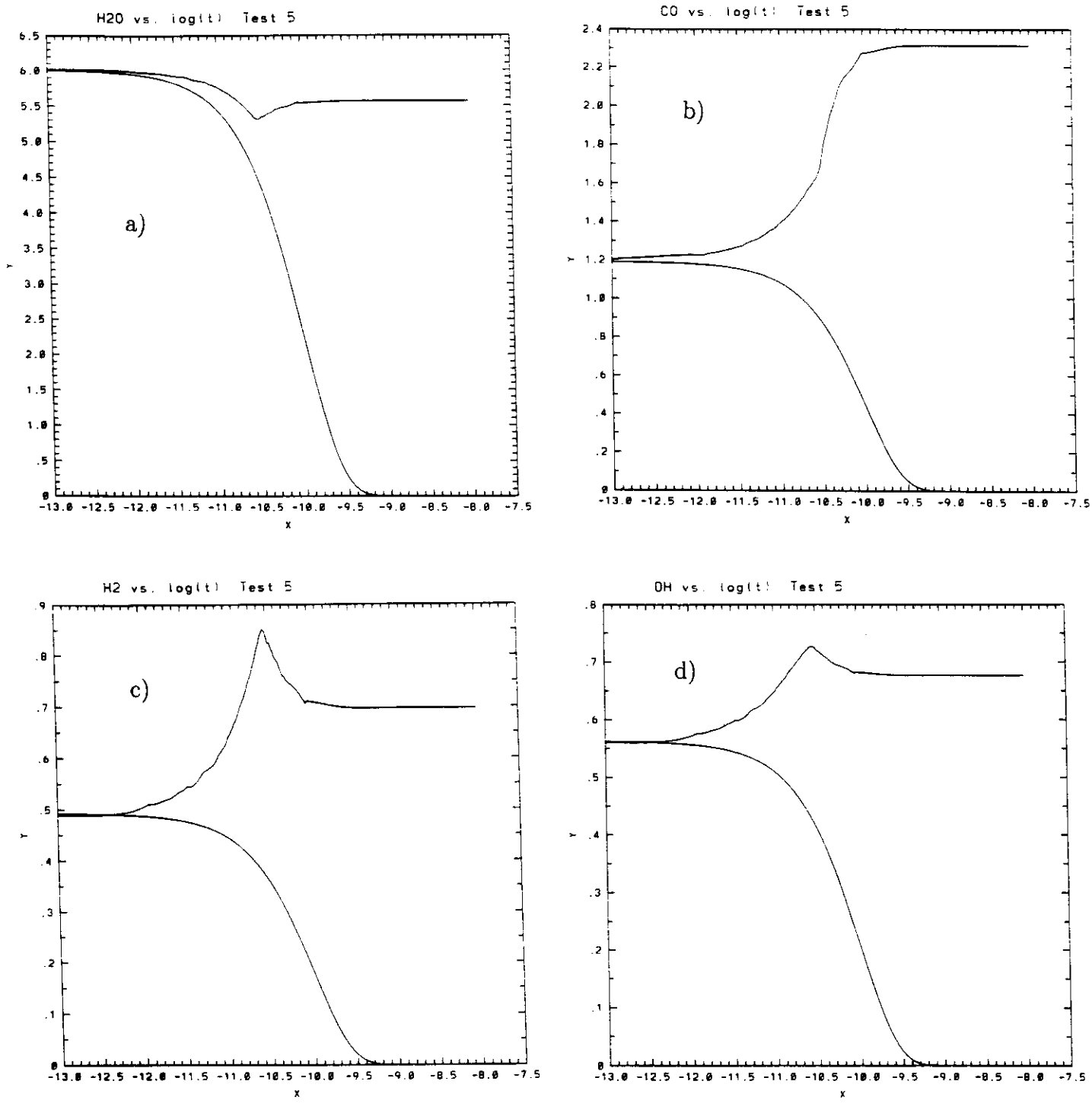

Fig. 8 Test 5, PSR ($\omega = 10^{10} s^{-1}$). Specific mole numbers x1,000 vs. $\log_{10}(t)$, where t is in seconds. Comparison of detailed kinetics and TGLDM. a) H_2O, b) CO, c) H_2, d) OH.